The ALS-associated KIF5A P986L variant is not pathogenic for Drosophila motoneurons

Sophie Layalle, Franck Aimond, Véronique Brugioti, Claire Guissart, Cédric Raoul, Laurent Soustelle

scientific reports

Check for updates

OPEN

The ALS-associated KIF5A P986L variant is not pathogenic for *Drosophila* motoneurons

Sophie Layalle[1✉], Franck Aimond[1], Véronique Brugioti[1], Claire Guissart[1,2], Cédric Raoul[1,3] & Laurent Soustelle[1✉]

Amyotrophic lateral sclerosis (ALS) is a devastating paralytic disorder caused by the death of motoneurons. Several mutations in the *KIF5A* gene have been identified in patients with ALS. Some mutations affect the splicing sites of exon 27 leading to its deletion (Δ27 mutation). KIF5A Δ27 is aggregation-prone and pathogenic for motoneurons due to a toxic gain of function. Another mutation found to be enriched in ALS patients is a proline/leucine substitution at position 986 (P986L mutation). Bioinformatic analyses strongly suggest that this variant is benign. Our study aims to conduct functional studies in *Drosophila* to classify the KIF5A P986L variant. When expressed in motoneurons, KIF5A P986L does not modify the morphology of larval NMJ or the synaptic transmission. In addition, KIF5A P986L is uniformly distributed in axons and does not disturb mitochondria distribution. Locomotion at larval and adult stages is not affected by KIF5A P986L. Finally, both KIF5A WT and P986L expression in adult motoneurons extend median lifespan compared to control flies. Altogether, our data show that the KIF5A P986L variant is not pathogenic for motoneurons and may represent a hypomorphic allele, although it is not causative for ALS.

Amyotrophic lateral sclerosis (ALS) is a fatal neurodegenerative disease that affects the motor system and is the most common adult-onset motoneuron disease[1]. ALS is characterized by the progressive dismantling of neuromuscular junctions (NMJs) and the degeneration of motoneurons in the brain and spinal cord. Motoneuron loss leads to progressive paralysis and death due to respiratory failure within 3 years of disease onset. Most cases of ALS are sporadic, with up to 10% classified as familial[2]. Currently, familial ALS-associated mutations have been found in approximately 40 causative genes[3–5].

The rise in the number of patients routinely tested has led to the identification of numerous variants associated with human diseases, presenting a significant challenge to molecular diagnostics[6]. With each newly discovered variant, questions about gene function and its role as a causative factor are repeatedly raised. To address this, bioinformatics tools are commonly used to predict whether the variant may affect gene function helping to classify it as benign or pathogenic[7]. However, these predictions need to be validated through functional studies conducted in model organisms, which can also help answer to these questions. For this reason, there is growing interest in using the nematode *Caenorhabditis elegans*, the fruit fly *Drosophila melanogaster* and the fish *Danio rerio* to help interpret data generated by next generation sequencing and bioinformatics approaches[8,9] .

In 2018, a genome-wide association study and whole exome sequencing have identified ALS-associated mutations in the *KIF5A* gene[10,11]. KIF5A belongs to the kinesin superfamily, which has 45 members in mammals sub-divided into 14 families[12]. KIF5A is a member of the Kinesin 1 family, along with KIF5B and KIF5C. While KIF5B is ubiquitously expressed, KIF5A and KIF5C are mainly expressed in neurons[13]. Members of the Kinesin 1 family are microtubule-dependent molecular motors that transport various cargos from the soma to the periphery. Kinesin 1 homodimerize and interact with a dimer of Kinesin light chain and adaptor proteins to transport mitochondria, mRNAs and organelles among others[14]. Several types of mutations in the *KIF5A* gene have been associated with ALS. First, a set of mutations has been described to affect the splicing sites of exon 27, leading to its deletion and the formation of a KIF5A mutant protein with a new C-terminal end (called KIF5A Δ27)[10,11,15–19]. Second, other mutations including missense and small deletions have been found in sporadic or familial ALS cases and remain to be characterized[10,11,15,19–25]. Among them, a single nucleotide polymorphism (SNP rs113247976, NM_004984.4(KIF5A):c.2957C > T) resulting in a Pro986Leu coding change within the

[1]Institute for Neurosciences Montpellier, Institut National de la Santé et de la Recherche Médicale, Université Montpellier, Montpellier, France. [2]Service de Biochimie et Biologie Moléculaire, CHU Nîmes, Université Montpellier, Nîmes, France. [3]ALS Reference Center, CHU Montpellier, Université Montpellier, Montpellier, France. ✉email: sophie.layalle@inserm.fr; laurent.soustelle@inserm.fr

C-terminal region of KIF5A (hereafter referred to as KIF5A P986L) was found to be enriched in ALS patients[10,11]. Several studies have demonstrated that KIF5A Δ27 mutations lead to a toxic gain of function. Our study, along with two others have demonstrated that the KIF5A Δ27 protein is prone to form toxic cytoplasmic inclusions[26–28]. It has also been described that Δ27 mutations can result in a constitutively active Kinesin by relieving its auto-inhibition[26,29]. Using negative-stain electron microscopy and crosslinking mass spectrometry, a more recent study has confirmed that KIF5A Δ27 is prone to aggregation but is still able to adopt the autoinhibited state, albeit with greater instability[30]. In *Drosophila*, KIF5A Δ27 expression in motoneurons induces alterations of morphology and synaptic transmission at larval NMJs, as well as impaired locomotion and motoneuron death[28]. In addition, numerous KIF5A Δ27-positive cytoplasmic inclusions are present in motoneuron axons, and are associated with disturbed mitochondria distribution[28]. While it is clear that KIF5A Δ27 is pathogenic for motoneurons, little is known about the KIF5A P986L variant.

Here, we conducted functional studies to assess the potential deleterious effects of the KIF5A P986L mutation on *Drosophila* motoneurons. The expression of KIF5A P986L in motoneurons did not result in any alteration in the morphology of NMJs or synaptic transmission when compared to control larvae. Conversely, larvae expressing KIF5A WT show an increase in axonal branch length at NMJs that are unable to respond correctly to sustained stimulations. In addition, KIF5A P986L presents a diffuse localization in motoneuron axons, similar to what is observed for KIF5A WT. Mitochondria distribution is not affected by KIF5A P986L, whereas they are more present in axons and absent at NMJs of larvae expressing KIF5A WT. Furthermore, KIF5A P986L does not affect locomotion in either larval or adult stages. Lastly, the restricted expression of both KIF5A WT and P986L in adults had a beneficial effect on median lifespan. Based on these findings, we conclude that KIF5A P986L is not pathogenic for *Drosophila* motoneurons and could be considered as a hypomorphic allele of KIF5A.

Results

KIF5A P986L, a variant associated with ALS

A large genome-wide association study (GWAS) involving 59 804 controls and 20 806 ALS cases found a significant association between the SNP rs113247976 NM_004984.4(KIF5A):c.2957C > T p.(Pro986Leu) and ALS[11]. However, the authors of this study could not definitively confirm that the KIF5A P986L missense variant was the primary risk factor, given the possibility of other variants in linkage disequilibrium. In parallel, another study found that the KIF5A P986L missense variant was significantly enriched in familial ALS patients compared to controls[10]. However, among the 29 ALS patients carrying the non-synonymous single nucleotide variant rs113247976, 11 were heterozygous for genetic variants in other genes associated with ALS[10]. This makes it difficult to conclude that only the KIF5A P986L variant is causative for ALS. Nevertheless, these studies highlight the rs113247976 SNP as the most prevalent genetic factor contributing to the development of ALS[10,11]. More recently, at least two studies have confirmed that the KIF5A P986L variant is reported at higher frequencies in ALS cohorts, leading them to conclude that harboring the KIF5A P986L variant represents an increased risk factor for ALS[17,18].

In the context of genetic diagnosis, using the American College of Medical Genetics and Genomics (ACMG) criteria[31], several molecular arguments strongly suggest the benign nature of the KIF5A P986L variant (Table 1). First, the variant's allele frequency in the gnomAD v4 exomes dataset is 1.24%, which exceeds the threshold derived from clinically reported variants in *KIF5A* (0.01%)[32], meeting the ACMG BS1 criteria. The variant is then observed in healthy adults, as indicated by an allele count of 19,694 in gnomAD v4, exceeding the threshold of 5 for the autosomal dominant gene *KIF5A,* in line with the ACMG BS2 criteria. Moreover, the ACMG BP4 criteria further supports its benign nature, as all queried in silico prediction software collectively predict the variant to be benign[33,34].

To gain a better understanding of the effects of KIF5A P986L and to gather in vivo evidence for its classification as pathogenic or benign, we used the *Drosophila* model, which is increasingly being used to characterize variants identified in various human diseases[8,9].

Expression of KIF5A P986L in motoneurons does not affect neuromuscular junction morphology

To determine whether the KIF5A P986L variant could be deleterious for *Drosophila* motoneurons, we first generated transgenic lines to overexpress it in a tissue-specific manner using the UAS/Gal4 system[35]. Western blot quantification was done to select transgenic lines with KIF5A expression levels similar to those of the wild-type (Fig. 1). The expression levels of KIF5A WT and P986L were also similar to those of KIF5A Δ27 (Fig. 1), allowing for the comparison of their effects when expressed in different tissues.

In a first attempt to monitor the effects induced by KIF5A P986L, we used the VGlut-Gal4 line to specifically target the motoneurons[36] and analyzed the morphology of larval NMJs. We used the anti-HRP antibody to label the neuronal membranes[37], and the active zones, which are the sites of neurotransmitter release, were labeled using the anti-Brp antibody[38] (Fig. 2a). We found that the expression of KIF5A P986L did not alter the length of axonal branches, the area of the NMJs, the number of active zones per NMJ or the number of active zones per bouton compared to the control condition (Fig. 2a–e). Interestingly, the expression of KIF5A WT in motoneurons induced an overgrowth phenotype with an increase of the length of axonal branches and the area of NMJs compared to control and KIF5A P986L-expressing larvae (Fig. 2a–e). These results indicate that KIF5A P986L, in contrast to KIF5A WT, does not affect NMJ morphology.

To investigate the presence of degenerating NMJs, we looked for ghost boutons by using the anti-Dlg (Discs large) antibody, which mostly labels the subsynaptic reticulum (SSR) in the postsynaptic muscles[39]. Indeed, the degeneration of motoneurons is characterized by the loss of presynaptic motoneuronal membranes that precedes the disassembly of the SSR[40], implying that degenerating NMJs retain the anti-Dlg staining but lose the anti-HRP.

ACMG evidence symbol	Category	Features	Values	Prediction	Description
BS1	Allele frequency is greater than expected for disorder	gnomAD v4 allele frequency (all)	0.0124	Benign	Threshold < 0.0001 for gene with autosomal dominant inheritance
BS2	Observed in a healthy adult individual for a dominant (heterozygous) disorder	gnomAD v4 allele count	19,694	Benign	Threshold < 5 allele counts for gene with autosomal dominant inheritance
BP4	Multiple lines of computational evidence suggest no impact on gene or gene product (conservation, evolutionary, splicing impact, etc.)	SIFT	0.29	Tolerated	Threshold < 0.05 for damaging—single score
		Polyphen 2 HumDiv	0.0	Benign	Thresholds ≥ 0.454|0.957 for possibly and probably damaging—single score
		Polyphen 2 HumVar	0.0	Benign	Thresholds ≥ 0.447|0.909 for possibly and probably damaging—single score
		Fathmm	−0.7	Tolerated	Threshold ≤ −1.5 for damaging—single score
		AlphaMissense	0.074	Likely benign	Thresholds 0.34|0.564 for likely benign, ambiguous, likely pathogenic—single score
		REVEL	0.142	Benign	Thresholds 0.2|0.5 for benign, uncertain, damaging—meta score
		ClinPred	0.007	Tolerated	Threshold ≥ 0.5 for damaging—meta score
		Meta SVM	−0.9125 (10)	Tolerated	Threshold ≥ 0 for damaging (reliability index: 0–10), 10: high—meta score
		Meta LR	0.0546 (10)	Tolerated	Threshold ≥ 0.5 for damaging (reliabilty index: 0–10), 10: high—meta score
		Mistic	0.34	Tolerated	Threshold ≥ 0.5 for damaging—meta score
		Franklin Genoox	0.143	Benign	Benign supporting 0–0.15, pathogenic supporting 0.7–0.8, pathogenic moderate 0.8–0.9, pathogenic strong 0.9–1.0—meta score
		Varsome MetaRNN	0.00402	Very strong benign	Threshold ≤ 0.00692 for very strong benign—meta score

Table 1. Combined molecular arguments provide evidence supporting the benign status of the KIF5A P986L variant.

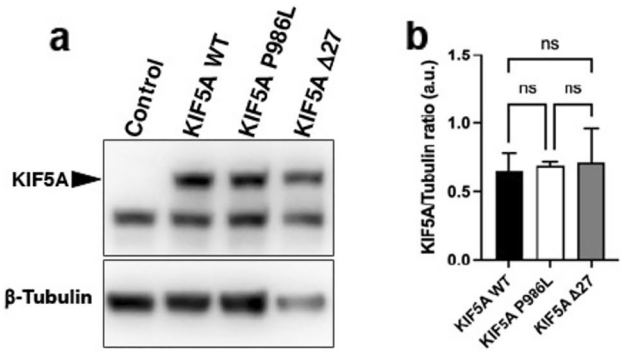

Fig. 1. Expression level of WT, P986L and Δ27 KIF5A proteins. (**a**) Representative immunoblots of protein extracts from thoraxes of control, KIF5A WT, KIF5A P986L and KIF5A Δ27-expressing flies using the VGlut-Gal4 motoneuron driver. KIF5A is indicated by a black arrowhead. Note the presence of a non-specific band in all genotypes. Anti-ß-Tubulin was used as a loading control. Western blots were cropped in this figure; full blots are shown in Supplementary Fig. 1. (**b**) Quantification of gel bands. Data are shown as means ± s.e.m. (a.u. arbitrary units, ns: not significant, ordinary one-way ANOVA with Tukey's multiple comparisons test, $n = 3$ gels).

As shown in Fig. 2f, we never observed ghost boutons since the HRP-positive presynaptic terminals consistently remained juxtaposed to the Dlg-positive postsynaptic SSR. This indicates that the postsynaptic compartment of NMJs is not affected by the expression of KIF5A P986L in motoneurons, similar to the observation made for KIF5A WT[28] (Fig. 2f).

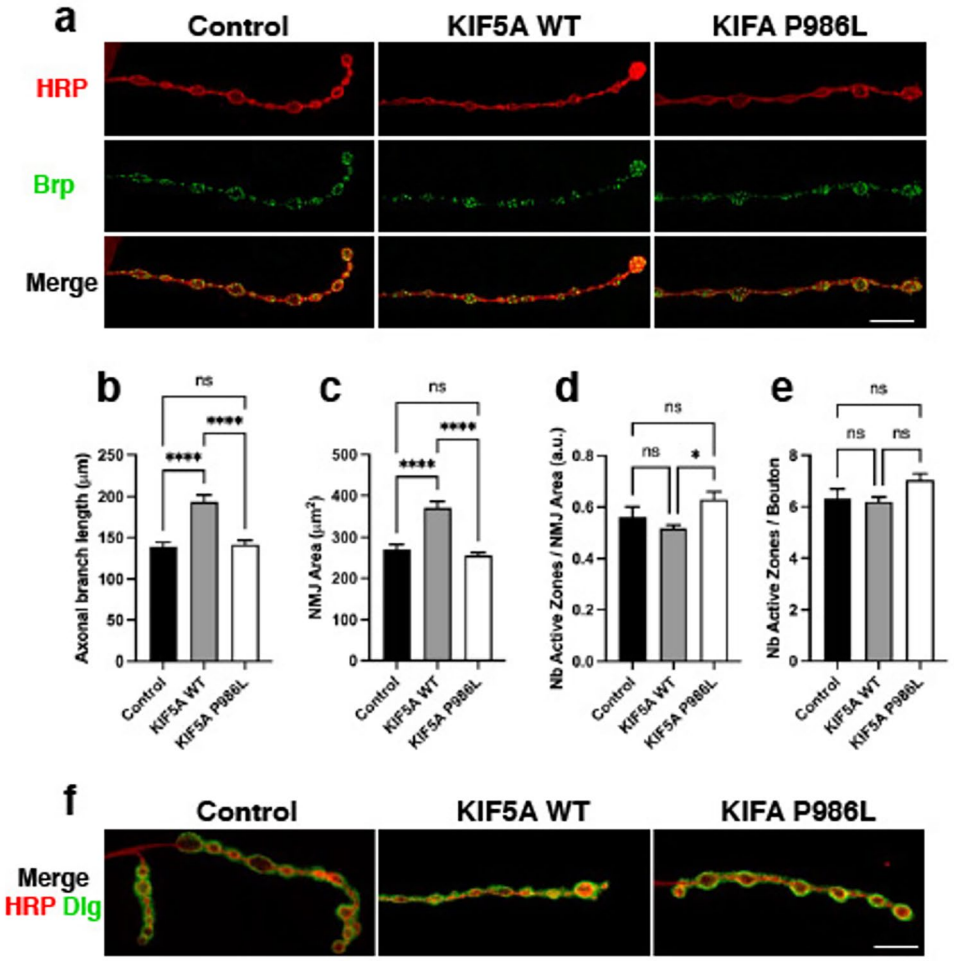

Fig. 2. The morphology of NMJs is not affected by KIF5A P986L. (**a**) Anti-HRP (red) and anti-Brp (green) labeling were used to visualize the presynaptic motoneuron endings and the active zones, respectively, in control, KIF5A WT and KIF5A P986L-expressing larvae using the VGlut-Gal4 motoneuron driver. Scale bar: 5 µm. (**b**–**e**) Quantification of axonal branch length (**b**), NMJ area (**c**), number of active zones per NMJ area (**d**) or per bouton (**e**). Note that all these parameters are unchanged by KIF5A P986L (white) compared to control (black), while KIF5A WT (grey) induces an increase in the length of axonal branches and NMJ area (ns: not significant, $p > 0.05$; *$p < 0.05$; ****$p < 0.0001$; ordinary one-way ANOVA with Tukey's multiple comparisons test; n = 10, 13 and 13 for control, KIF5A WT and KIF5A P986L, respectively). (**f**) Anti-HRP (red) and anti-Dlg (green) antibodies were used to label the presynaptic motoneuron endings and the postsynaptic density, respectively, in control, KIF5A WT and KIF5A P986L-expressing larvae by using the VGlut-Gal4 motoneuron driver. Note that the presynaptic endings and postsynaptic densities are closely apposed for all genotypes. Scale bar: 5 µm.

Synaptic transmission and locomotion are not altered by the KIF5A P986L variant

To evaluate the potential impact of KIF5A P986L on motoneuron physiology, we analyzed synaptic transmission at larval NMJs. We found that the expression of KIF5A P986L does not affect the amplitude and frequency of miniature excitatory junction potentials (mEJPs) compared to control and KIF5A WT-expressing larvae (Fig. 3a–c). Additionally, the amplitude of evoked excitatory junction potentials (eEJPs) as well as the quantal content were found to be similar between control, KIF5A WT and KIF5A P986L-expressing larvae (Fig. 3a, d, e). These results indicate that spontaneous and evoked release of synaptic vesicles remains unaffected by the expression of KIF5A P986L in motoneurons. We then investigated whether NMJs could respond correctly to high frequency stimulation by applying a train of 100 stimulations at a frequency of 20 Hz. Expression of KIF5A P986L did not alter the amplitude of the second or 100th stimulation compared to the control (Fig. 3f, g). In contrast, both the second and 100th responses were reduced with KIF5A WT expression (Fig. 3f, g), indicating that expression of KIF5A WT and P986L leads to distinct effects on NMJs when subjected to high frequency stimulation.

We next asked whether the expression of KIF5A P986L in motoneurons could affect larval locomotion. Larvae were placed on a petri dish and their locomotor behavior, i.e., the distance travelled during a 2-min period was measured. As shown in Fig. 3h, KIF5A WT-expressing larvae display a reduced locomotion compared to the control group. This reduction in locomotion can be attributed to the abnormal NMJ morphology and

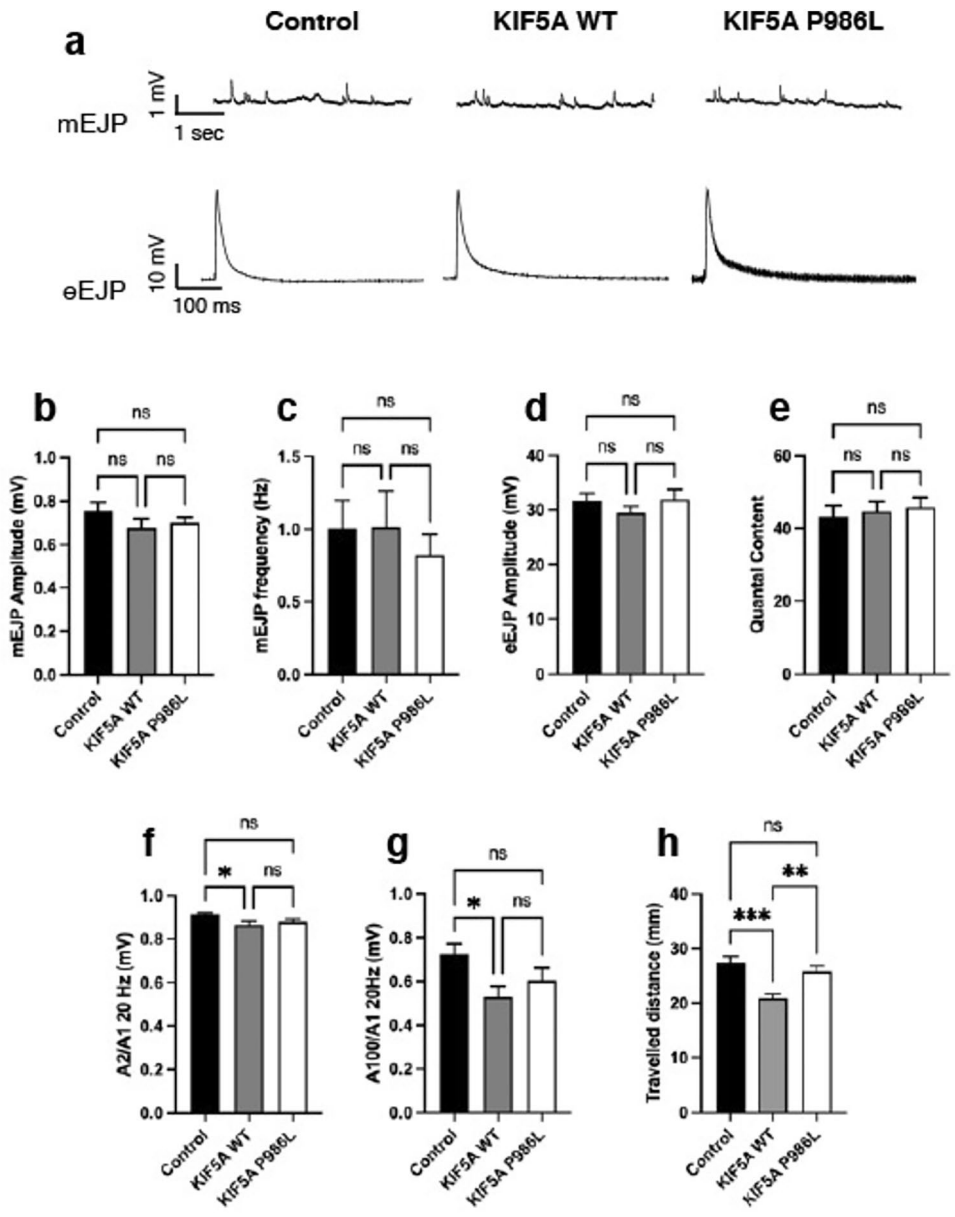

Fig. 3. The synaptic transmission at NMJs and larval locomotion are not altered by KIF5A P986L. (**a**) Representative traces of mEJPs (top) and eEJPs (bottom) obtained from control, KIF5A WT and KIF5A P986L-expressing larvae using the VGlut-Gal4 motoneuron driver. (**b,c**) Amplitude (**b**) and frequency (**c**) of mEJPs. (**d**) Amplitude of eEJPs. (**e**) Quantal content calculated by dividing the mean of eEJPs by the mean of mEJPs. (**f,g**) A train of 100 stimulations at a frequency of 20 Hz was applied to NMJs. The A2/A1 (**f**) and the A100/A1 (**g**) ratio compare the amplitude of the first response (A1) to the second (A2) or to the 100th (A100), respectively. Note that KIF5A P986L-expressing larvae give rise to similar results as control. Contrary to KIF5A P986L, KIF5A WT-expressing larvae show a reduction of the second (**f**) or the hundredth (**g**) response compared to the first one. (**b–g**) ns: not significant, $p > 0.05$; $^{*}p < 0.05$; Kruskal–Wallis with Dunn's multiple comparisons test (**b**) or ordinary one-way ANOVA with Tukey's multiple comparisons test (**c–g**); $n = 11$, 12 and 11 for control, KIF5A WT and KIF5A P986L, respectively. (**h**) Quantification of the distance travelled by control, KIF5A WT and KIF5A P986L-expressing larvae by using the VGlut-Gal4 motoneuron driver. Note that unlike to KIF5A WT, KIF5A P986L does not reduce the distance travelled compared to the control ($^{**}p < 0.01$; $^{***}p < 0.001$; Kruskal–Wallis with Dunn's multiple comparisons test; $n = 30$ for each genotype).

activity-dependent fatigue we previously described. However, the distance travelled by KIF5A P986L-expressing larvae is higher than that of KIF5A WT-expressing larvae and is similar to the control condition (Fig. 3h). This indicates that KIF5A P986L does not cause defects in larval locomotion. Importantly, as reported for KIF5A Δ27-expressing larvae[28], we never observed a 'tail-flip' phenotype during larval crawling when KIF5A P986L

was expressed in motoneurons. Since the tail-flip phenotype is a hallmark of axonal transport defects[41,42], this strongly suggests that the axonal transport machinery is functional in larvae expressing the KIF5A P986L variant.

Mitochondria distribution is not affected by the expression of KIF5A P986L in motoneurons

Mitochondria are the most well-known cargo of KIF5A[43]. We have previously shown that the expression of KIF5A Δ27 leads to the aggregation of mitochondria in *Drosophila* motoneurons[28]. To determine whether the distribution of mitochondria could be affected by KIF5A P986L, we used the Mito-GFP reporter line, in which a mitochondrial import sequence is fused to GFP[44]. This allowed to visualize fluorescent mitochondria in motoneurons. Under control condition, the distribution of mitochondria in motoneuron axons were found to be uniform (Fig. 4a, c). This uniform distribution extended up to the NMJs (Fig. 4b, d). Consistent with our previous findings, expression of KIF5A WT in motoneurons induced an increase of mitochondria in the axons and a reduction at the NMJs (Fig. 4)[28]. Interestingly, expression of KIF5A P986L did not influence the localization of mitochondria, which were found in the axons and NMJs as observed in the control group (Fig. 4). Importantly, we did not observe aggregated mitochondria in larvae expressing either KIF5A WT or P986L (Fig. 4).

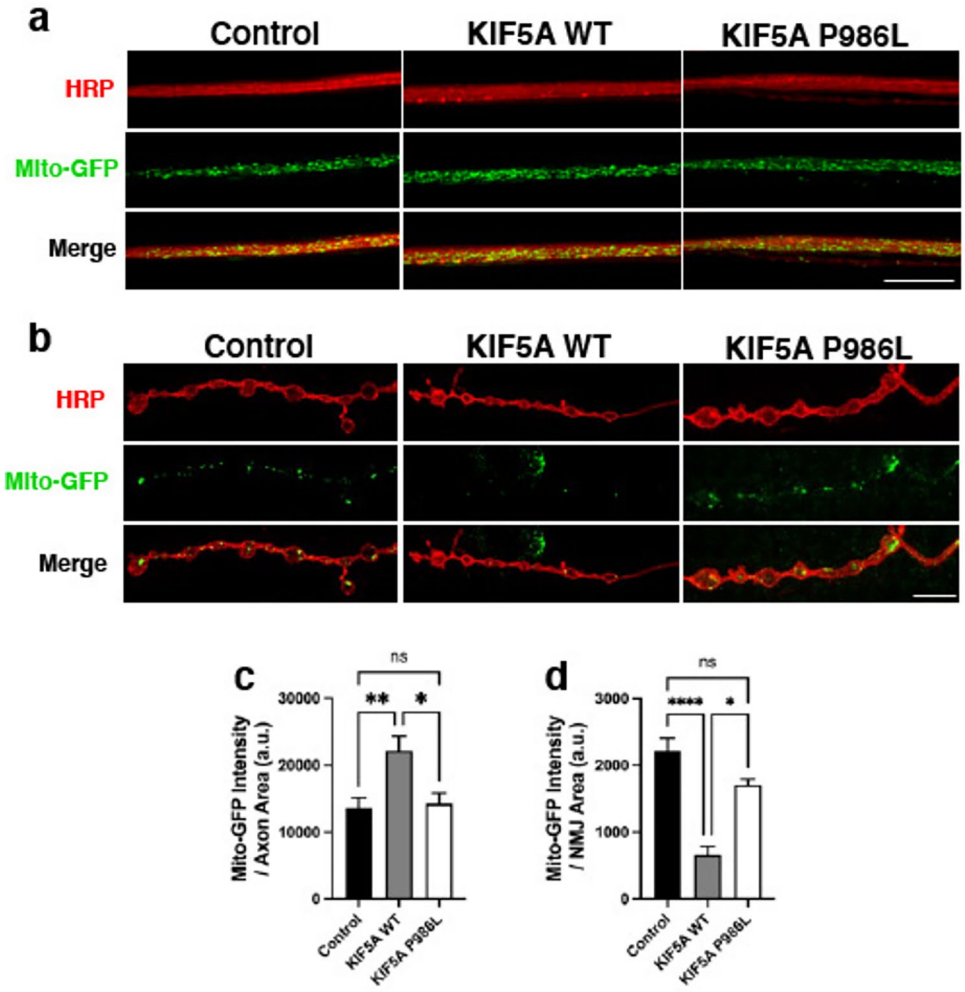

Fig. 4. Mitochondria distribution is not affected by KIF5A P986L. (**a,b**) Anti-HRP (red) and anti-GFP (green) labeling was used to visualize the motoneuron axons (red in (**a**)) or presynaptic endings (red in (**b**)) and mitochondria (green in (**a,b**)), respectively, in control, KIF5A WT and KIF5A P986L-expressing larvae using the VGlut-Gal4 motoneuron driver associated with the UAS-Mito-GFP reporter. (**a**) Note that mitochondria are enriched in axons of KIF5A WT-expressing larvae compared to control and KIF5A P986L-expressing larvae, which show a similar distribution. Scale bar: 10 µm. (**b**) Mitochondria are present at NMJs in control and KIF5A P986L-expressing larvae, but at lower levels in KIF5A WT-expressing larvae. Scale bar: 5 µm. (**c,d**) Quantification of mitochondria fluorescence intensity in the axons (**c**) and at NMJs (**d**); a.u. arbitrary units, ns: not significant, $p > 0.05$; $^{*}p < 0.05$; $^{**}p < 0.01$; $^{****}p < 0.0001$; Kruskal–Wallis with Dunn's multiple comparisons test. (**c**) $n = 13$, 10 and 8 for control, KIF5A WT and KIF5A P986L, respectively. (**d**) $n = 10$, 8 and 11 for control, KIF5A WT and KIF5A P986L, respectively.

KIF5A P986L is uniformly distributed in motoneuron axons

The rs113247976 SNP is located in exon 26 of KIF5A and, like the Δ27 mutations, affects the C-terminal region of the kinesin. Given the high propensity of KIF5A Δ27 to form aggregates[26–28], we asked whether the P986L mutation could affect the distribution of KIF5A. Immunostaining experiments showed no difference in the distribution of KIF5A WT and P986L, as both were uniformly found in motoneuron axons (Fig. 5a). Consistent with this, Carrington and collaborators observed that both KIF5A WT and P986L exhibited a diffuse localization into COS7 cells, whereas KIF5A Δ27 formed aggregates[30]. Previously, we observed that a small percentage of motoneuron axons contained small inclusions of KIF5A WT[28]. We confirm this observation (Fig. 5b), which has also been reported by other teams showing that KIF5A has a high propensity to oligomerize *in vitro*[45] and forms few cytoplasmic granules in a small number of transfected mammalian cell lines[26]. Based on this, we quantified the number of nerves containing cytoplasmic inclusions of KIF5A P986L. We found that approximately one third of nerves contain small KIF5A P986L-positive inclusions (Fig. 5b), which is similar to what was observed with KIF5A WT (Fig. 5b). In contrast, most, if not all, nerves expressing KIF5A Δ27 showed cytoplasmic inclusions (Fig. 5b). Thus, the distribution of KIF5A WT and P986L is similar in vivo, indicating that KIF5A localization is not affected by the P986L mutation.

KIF5A P986L is not detrimental in adult motoneurons

Since the previous experiments were performed at the larval stage, we wanted to investigate whether the expression of KIF5A P986L in adult motoneurons could affect locomotion in *Drosophila*. To induce the expression of KIF5A selectively in motoneurons during the early stage of adult life, we used the TARGET system[46]. Subsequently, 10- and 20-day-old flies were tested for climbing ability. At 10 days of age, the locomotion of control flies was similar to that of KIF5A WT-expressing flies (Fig. 6a), confirming that KIF5A WT expression does not affect adult locomotion. In contrast, KIF5A Δ27-expressing flies, used as a positive control, showed reduced

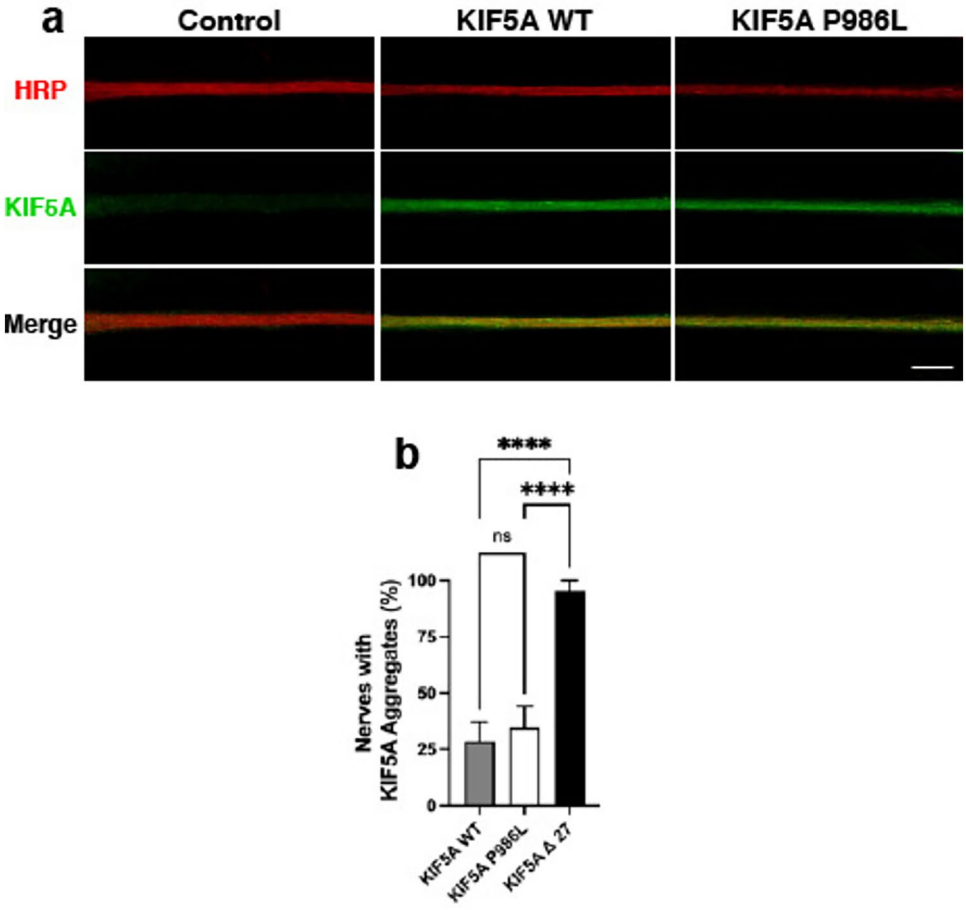

Fig. 5. KIF5A WT and P986L are uniformly distributed in motoneuron axons. (**a**) Anti-HRP (red) and anti-KIF5A (green) antibodies were used to label the motoneuron axons (red) and KIF5A protein (green), respectively, in control, KIF5A WT and KIF5A P986L-expressing larvae using the VGlut-Gal4 motoneuron driver. Note that KIF5A WT and P986L are uniformly distributed along the axons. Scale bar: 10 µm. (**b**) Quantification of motoneuron axons containing KIF5A-positive aggregates (ns: not significant, $p > 0.05$; ****$p < 0.0001$; Kruskal–Wallis with Dunn's multiple comparisons test. $n = 28$, 26 and 22 for KIF5A WT, P986L and Δ27, respectively).

locomotion (Fig. 6a). This was not observed in KIF5A P986L-expressing flies, which had similar performances to control and KIF5A WT-expressing flies (Fig. 6a). As expected, due to aging effects, the locomotion of control, KIF5A WT or P986L-expressing flies was reduced compared to 10 days, but no significant difference was observed between these three genotypes at 20 days (Fig. 6a). In contrast, KIF5A Δ27-expressing flies had died at this time point (Fig. 6a).

Generally, motoneuron dysfunction is associated with a reduced lifespan[47]. To definitively conclude that KIF5A P986L is not detrimental to motoneuron function, we analyzed the lifespan of flies with an adult-restricted expression of KIF5A. As shown in Fig. 6b, KIF5A Δ27 flies showed a reduced survival rate compared to control flies, as expected[28]. In contrast, both KIF5A WT and P986L-expressing flies showed an increase in median lifespan compared to control flies (Fig. 6b). These results indicate that the expression of the P986L variant of KIF5A is not toxic to motoneuronal function and that both the variant and the WT form are able to significantly increase the median life expectancy of flies.

Discussion

The primary objective of our study was to provide biological evidence regarding the potential pathogenicity of the KIF5A P986L variant, which has been found to be more prevalent in ALS patients[10,11,17,18]. For this purpose, we used a *Drosophila* model that specifically expresses this variant in motoneurons. This tissue-specific overexpression strategy has been increasingly used in the last decade to assess the functional impact of genetic variants[48]. Previously, this strategy allowed us to show that KIF5A Δ27 is pathogenic to motoneurons due to a toxic gain of function[28].

In the present work, we showed that the expression of KIF5A P986L had no significant effect on the morphology, the basal synaptic transmission at NMJs, or the locomotion of larvae when compared to the control condition. Furthermore, when KIF5A P986L expression was restricted to motoneurons during the adult stage, the climbing ability of these flies was similar to that of the control group. Altogether, these findings indicate that KIF5A P986L does not exert a significant detrimental effect on *Drosophila* motoneuron physiology.

When KIF5A WT was expressed in motoneurons, the length of axonal branches and the resulting area of NMJs were increased. Additionally, high frequency stimulations revealed that KIF5A WT expression

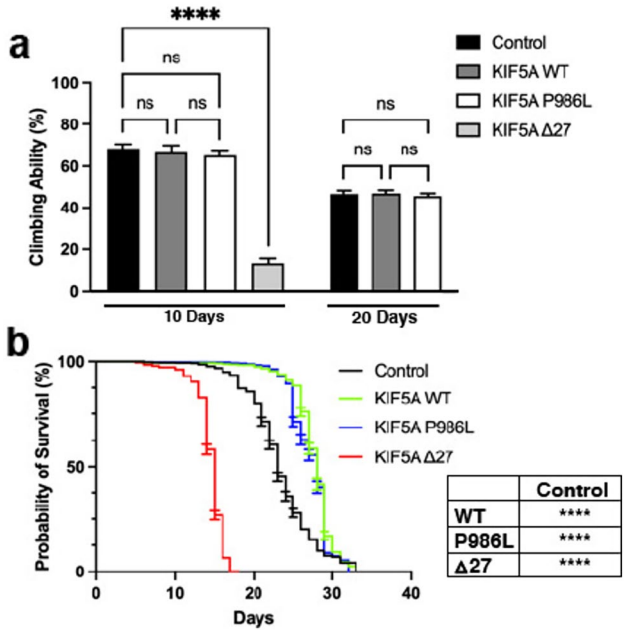

Fig. 6. Expression of KIF5A P986L in adult motoneurons does not affect climbing ability and lifespan. (**a**,**b**) Crosses were maintained at 18 °C and males were transferred at 29 °C immediately after eclosion to induce KIF5A expression only at the adult stage. Note that the KIF5A Δ27-expressing males were used as a control to confirm their reduced climbing ability and reduced survival. (**a**) Quantification of the climbing ability of control, KIF5A WT, KIF5A P986L and KIF5A Δ27-expressing male flies using the VGlut-Gal4 motoneuron driver combined with the tub-Gal80^{ts} transgene. As expected, the climbing ability of all flies decreases with age. Note that at 20 days, all flies expressing KIF5A Δ27 had died. However, the climbing performance was similar between control (black), KIF5A WT (dark grey) and KIF5A P986L (white) expressing flies at 10- and 20 days of age (ns: not significant, $p > 0.05$; ****$p < 0.0001$; ordinary one-way ANOVA with Tukey's multiple comparisons test; at ten days $n = 10$, 14, 22 and 14 for control, KIF5A WT, P986L and Δ27, respectively. At 20 days $n = 40$, for all genotypes). (**b**) Lifespan analysis of control (black), KIF5A WT (green), KIF5A P986L (blue) and KIF5A Δ27 (red) expressing male flies using the VGlut-Gal4 motoneuron driver combined with tub-Gal80^{ts} transgene. The median survival is 23, 28, 28 and 15 for control, KIF5A WT, P986L and Δ27, respectively [****$p < 0.0001$; Log-rank (Mantel-cox) test; $n = 443$, 343, 313 and 444 for control, KIF5A WT, P986L and Δ27, respectively].

prevented sustained response from NMJs, consistent with the observed lack of mitochondria at NMJs. Indeed, it is well-established that synaptic mitochondria are essential for normal neurotransmission during prolonged stimulation[49,50]. These defects may explain the reduced distance travelled by KIF5A WT-expressing larvae compared to control larvae. Interestingly, these phenotypes were not observed when KIF5A P986L was expressed, suggesting a loss-of-function allele since it does not induce the same effects as the wild-type form. However, when KIF5A P986L expression was restricted to adult motoneurons, the median lifespan of the flies increased significantly compared to the control group, similar to what was observed for KIF5A WT. This suggests that KIF5A P986L retains some of the wild-type function of KIF5A. From all these results, it is plausible to consider KIF5A P986L as a hypomorphic allele.

KIF5 proteins are known to transport a wide variety of cargos including protein-containing vesicles, tubulin oligomers, mitochondria, lysosomes, neurofilaments and mRNAs (for reviews see[51,52]). Our data suggest that KIF5A P986L does not have a significant impact on axonal transport. Three arguments support this hypothesis. First, the distribution of mitochondria, a known cargo of KIF5A[43,53], was not affected in KIF5A P986L-expressing larvae. Second, these larvae did not exhibit a tail-flip phenotype, which is easily observable when the posterior part of the larva rises up during crawling[54]. The tail-flip phenotype is characteristic of axonal transport defects and has been observed in *Drosophila* carrying mutated molecular motors or proteins that affect microtubule dynamic[54]. It is important to note that KIF5A Δ27 induces this phenotype when expressed in *Drosophila* motoneurons[28], confirming that the P986L mutation does not impact axonal transport compared to Δ27 mutation. Third, flies expressing KIF5A P986L show an extended median lifespan, which seems inconsistent with axonal transport alterations. Since the P986L substitution is located in the tail domain of the kinesin, which is responsible for cargo binding[51,52], it is possible that some cargos may not be transported efficiently within motoneurons. This hypothesis would reconcile the observed discrepancies between the phenotypes induced by the expression of KIF5A WT or P986L. Future studies will be necessary to confirm this hypothesis, which represents a major challenge considering the plethora of cargos transported by KIF5A.

From our study, we can conclude that the KIF5A P986L variant by itself is not causative for ALS, which supports the benign status of this variant according to the ACMG criteria. However, the involvement of this hypomorphic allele in the disease cannot totally be excluded. Indeed, as was previously suggested, the KIF5A P986L variant may be involved in the digenic/polygenic inheritance of the disease[10,17,18]. For example, one could speculate that the rs113247976 SNP might co-segregate with mutations in ALS-associated genes known to play a role in cytoskeleton dynamics. In addition to *KIF5A*, this group of genes includes *ALS2*, *DCTN1*, *PFN1*, *NF-L*, *NF-H*, *PRPH*, *SPAST*, and *TUBA4A* (for reviews see[55,56]). The oligogenic/polygenic inheritance of the rs113247976 SNP may also occur with other ALS-associated genes, as mutations in some of them have been described to affect the cytoskeleton dynamics, such as mutations in *FUS*[57], *TARDBP*[58], *SOD1*[59,60] and *C9ORF72*[61]. Exploring all the possibilities and identifying the variants associated with KIF5A P986L that may lead to ALS will demand considerable effort. However, there is an increasing interest in the oligogenic/polygenic inheritance in ALS, as mendelian inheritance only accounts for only a small fraction of cases[62,63]. In the future, there is no doubt that this area of research will bring new knowledge on the molecular causes of ALS, allowing to design original therapeutic strategies. Nonetheless, at present, the complexity introduced by risk factors or polygenic inheritance patterns complicates genetic counseling. For instance, the presence of a heterozygous variant such as KIF5A P986L neither ensures nor singularly precipitates the disease. Communicating the presence of such polymorphisms could potentially cause unwarranted distress for patients and their families, without providing any clear benefits. Genetic counseling is only feasible for variants with clearly established pathogenicity. In this regard, having reliable functional tests to assess variants proves immensely helpful in diagnosis.

In this way, demonstrating that a variant is not causative for a disease may seem irrelevant. However, it is crucial to classify both non-causative and causative variants in order to provide a molecular diagnostic for patients who want to understand the reasons for their illness. Finally, the development and effectiveness of new therapeutic strategies, such as antisense oligonucleotides targeting the disease-associated allele[64], depend heavily on the classification of genetic variants. This treatment would not be possible if the identified variant is not pathogenic, highlighting the importance of variant classification for each patient. In the future, biological systems, including simple organisms, ex-vivo cultures, or cell line cultures, will need to be further refined to address the large number of variants found in patients.

Methods

Drosophila stocks and husbandry

Drosophila stocks were raised on standard cornmeal medium under temperature-controlled conditions. Experiments were performed at 25 °C on both males and females unless stated otherwise. The control strain was w^{CS} (w^{1118} flies outcrossed with CantonS for 10 generations). For each experiment, control condition was the progeny of the VGlut-Gal4 line crossed with the w^{CS} strain. The VGlut-Gal4 (OK371-Gal4, #26160), UAS-Mito-GFP (#8443) and tub-$Gal80^{ts}$ (#7017) stocks were obtained from the Bloomington Stock Center. For the longevity assay, all the stocks used were backcrossed into a w^{CS} background for six generations. For the UAS-KIF5A transgenic lines, full-length cDNAs of the WT, P986L and Δ27 human KIF5A were synthetized (Gene Universal, USA) and cloned into a pcDNA3.1(+) plasmid. After subcloning of the cDNAs into the pUAST vector, random transgenesis was performed by BestGene Inc (Chino Hills, CA, USA). UAS-KIF5A WT and Δ27 lines were already described in[28].

Western blot

Protein extracts were prepared from adult thoraces of 2/3-day-old *Drosophila* expressing KIF5A under the control of the VGlut-Gal4 driver. Cell homogenization and lysis were done in RIPA buffer (150 mM sodium chloride, 1%

NP-40, 0.5% sodium deoxycholate, 0.1% SDS, 50 mM Tris, pH 8.0, supplemented with protease inhibitor cocktail, Roche Life Science, Switzerland) for 2 h at room temperature. Laemmli buffer was then added and the samples were boiled for 5 min. Samples were analyzed by SDS-PAGE using Mini-PROTEAN TGX precast gels (Bio-Rad). Separated proteins were transferred onto nitrocellulose membranes using Trans-Blot Turbo (Bio-Rad, USA). Primary and secondary antibodies were incubated in 5% milk in PTX (PBS, 0.1% Triton X-100), and washed with PTX. The following primary antibodies were used: mouse anti-KIF5A (1/1000, Santa Cruz Biotechnology, USA, sc-376452), mouse E7 (1/400, anti-β tubulin from the Developmental Studies Hybridoma Bank, DSHB, maintained at the University of Iowa, USA). HRP-linked goat anti-mouse (1/10.000, Jackson ImmunoResearch Laboratories, UK) was used as secondary antibody. Immunodetection was done using the ClarityWestern ECL kit (Bio-Rad, USA). Chemiluminescence detection was acquired using the Fusion Fx system (VILBER, France). Quantification of gel bands was done by using Fiji software (Analyze gels).

Immunostaining and imaging

Wandering third instar larvae were dissected in PBS, 1 mM EDTA and fixed in 4% EM-grade paraformaldehyde (Fisher Scientific, France) in PBS for 20 min at room temperature. Primary antibodies were incubated overnight in PBS 0.3%Triton, 1% BSA at 4 °C at the following dilutions: mouse anti-Brp (NC82): 1/100, mouse Dlg (4F3): 1/100; obtained from DSHB, USA. Rabbit anti-GFP (A-11122, Invitrogen, France): 1/1000, goat anti-HRP Cy3 (Jackson ImmunoResearch Laboratories, USA): 1/800; mouse anti-KIF5A (Santa Cruz Biotechnology, USA, sc-376452): 1/500. Corresponding secondary antibodies were incubated for 2 h at room temperature: AlexaFluor-594 donkey anti-mouse and AlexaFluor-488 donkey anti-rabbit (Fisher Scientific, France) were used at 1/800 dilution. The final preparations were mounted in 80% glycerol.

Imaging was performed on a Zeiss LSM880 Airyscan confocal microscope with a 63X Plan Apo 1.4 numerical aperture objective or on a Zeiss Apotome Axio Imager for experiments using Mito-GFP. For each experimental set, images were collected using identical imaging and processing parameters. The z stacks were processed and analyzed using Fiji (National Institutes of Health). Representative images are the maximum projection z stacks; brightness and contrast were adjusted in Adobe Photoshop 2022 (Adobe System). Analysis of NMJ morphology was performed on muscle 4 in segments A3-A5. NMJ area and axonal length were quantified using Fiji software and NeuronJ plugin, respectively, while the number of Brp puncta was manually counted. Mitochondrial fluorescence intensity was quantified on z-stacks converted to maximum intensity projection using Fiji. Delineation of the axonal portions or synaptic terminals representing the area of interest was performed on HRP staining. A threshold mask was applied to the GFP staining and the RawIntDen representing the total intensity of the GFP (Mito-GFP) signal, was calculated. The GFP intensity per unit area was then normalized.

Electrophysiology

Electrophysiological recordings were obtained from wandering third instar larvae, as previously described[65]. To avoid muscular contraction, larvae were dissected in "free-Ca^{2+}" HL3.1 solution (70 mM NaCl, 5 mM KCl, 4 mM MgCl2, 10 mM NaHCO3, 5 mM trehalose, 115 mM sucrose, 5 mM HEPES, pH 7.2). Then, electrophysiological experiments were done on larvae infused with HL3.1 solution containing 1 mM Ca^{2+}. To apply local stimulation, the cut end axon was sucked into a patch pipet (resistance ~ 1 MΩ). Recordings from muscle 6, segment A3, were obtained with electrodes of a resistance of 30–40 MΩ filled with 3 M KCl, using an Axon Multiclamp 700B amplifier (Molecular Devices, USA). Only muscles presenting a resting membrane potential < −60 mV and an input resistance of ≥ 5 MΩ were considered. Data were analyzed using Clampfit. For electrophysiological protocols: miniature excitatory junction potentials (mEJP) were recorded at resting potential for 3 min without any stimulation. From these recordings, resting potential, mEJP amplitude and frequency were determined. Evoked excitatory junction potentials (eEJPs) were obtained by applying 10 stimulations every 6 s, at voltage sufficient to induce muscle evoked responses (1–3 mV). An average of these recordings was obtained to determine eEJP amplitude. Then, dividing the average amplitude of eEJPs by the average amplitude of mEJPs was done to obtain the quantal content. Paired-pulse stimuli protocols, consisting of applying 2 consecutive pulses (at 20 Hz), were performed to study synaptic facilitation. Quantification was obtained by dividing the amplitude of the second eEJP (A2) by the amplitude of the first eEJP (A1). Activity-dependent fatigue of neurotransmitter release was studied by recording multipulse protocol of 100 consecutive stimulations (at 20 Hz). Quantification was obtained by dividing the amplitude of the last eEJP (A100) by the amplitude of the first eEJP (A1).

Larval locomotion

The protocol was previously described by[66]. Briefly, third instar larvae were placed in the centre of a Petri dish filled with grape juice agar. Larval locomotion was video-recorded for 2 min using a camera (Sony HDR-CX240), and movies were analyzed using the Fiji plugin manual tracking to calculate the distance travelled.

Climbing assay and lifespan analysis

For the climbing assay and lifespan analysis, the VGlut-Gal4; tub-$Gal80^{ts}$ strain was crossed with the different UAS-KIF5A or w^{CS} control strains and maintained at permissive temperature (18 °C) until hatching. Males were then collected and maintained at 29 °C to induce KIF5A expression.

For each climbing test, ten males at 10 or 20 day-old were placed in 25 ml Falcon pipette and allowed to recover. Each pipette was tested by gently tapping the flies to the bottom, and the number of flies that climbed above the 12 cm mark within 30 s was counted. After a rest period of 2 min, the assay was repeated once. The number of flies that passed the 12 cm mark was expressed as a percentage of the total number of flies.

For lifespan, 20 males of each genotype were collected per tube and placed at 29 °C to age. The number of dead flies was then counted every 2–3 days as they were transferred to fresh food.

Experimental design and statistical analyses

For all experiments, the control and experimental genotypes were tested simultaneously. In all figures, data are shown as mean ± s.e.m., the statistical test used to analyze the data and the number of samples tested (n) are given in the figure legends as well as the *p* value for each test. All statistical analyses were performed using GraphPad Prism (version 9). Values were tested for normal distribution using the D'Agostino and Pearson test. Multiple comparisons were done by using ordinary one-way ANOVA with Tukey's multiple comparisons test. For non-parametric values, a Kruskal–Wallis with Dunn's multiple comparisons test was applied. For the longevity assays, Kaplan–Meier survival curves were generated, and significant differences were assessed based on the Log-rank (Mantel-cox) test (Supplementary Information).

Data availability

Most data generated during this study are included in this published article and its supplementary information file. Any additional inquiries are available upon request to the corresponding authors.

Received: 16 June 2024; Accepted: 16 August 2024
Published online: 22 August 2024

References

1. Talbott, E. O., Malek, A. M. & Lacomis, D. The epidemiology of amyotrophic lateral sclerosis. *Handb. Clin. Neurol.* **138**, 225–238 (2016).
2. Gros-Louis, F., Gaspar, C. & Rouleau, G. A. Genetics of familial and sporadic amyotrophic lateral sclerosis. *Biochim. Biophys. Acta* **1762**, 956–972 (2006).
3. Mejzini, R. *et al.* ALS genetics, mechanisms, and therapeutics: Where are we now?. *Front. Neurosci.* **13**, 1310 (2019).
4. Shatunov, A. & Al-Chalabi, A. The genetic architecture of ALS. *Neurobiol. Dis.* **147**, 105156 (2021).
5. Wang, H., Guan, L. & Deng, M. Recent progress of the genetics of amyotrophic lateral sclerosis and challenges of gene therapy. *Front. Neurosci.* **17**, 1170996 (2023).
6. Lupski, J. R., Belmont, J. W., Boerwinkle, E. & Gibbs, R. A. Clan genomics and the complex architecture of human disease. *Cell* **147**, 32–43 (2011).
7. Spielmann, M. & Kircher, M. Computational and experimental methods for classifying variants of unknown clinical significance. *Cold Spring Harb. Mol. Case Stud.* **8**, a006196 (2022).
8. Baldridge, D. *et al.* Model organisms contribute to diagnosis and discovery in the undiagnosed diseases network: Current state and a future vision. *Orphanet. J. Rare Dis.* **16**, 206 (2021).
9. Yamamoto, S., Kanca, O., Wangler, M. F. & Bellen, H. J. Integrating non-mammalian model organisms in the diagnosis of rare genetic diseases in humans. *Nat. Rev. Genet.* **25**, 46–60 (2024).
10. Brenner, D. *et al.* Hot-spot KIF5A mutations cause familial ALS. *Brain* **141**, 688–697 (2018).
11. Nicolas, A. *et al.* Genome-wide analyses identify KIF5A as a novel ALS gene. *Neuron* **97**, 1268-1283.e6 (2018).
12. Miki, H., Setou, M., Kaneshiro, K. & Hirokawa, N. All kinesin superfamily protein, KIF, genes in mouse and human. *Proc. Natl. Acad. Sci. USA* **98**, 7004–7011 (2001).
13. Kanai, Y. *et al.* KIF5C, a novel neuronal kinesin enriched in motor neurons. *J. Neurosci.* **20**, 6374–6384 (2000).
14. Hackney, D. D. & Twelvetrees, A. E. The kinesin-1 family: Long-range transporters. In *The Kinesin Superfamily Handbook* (CRC Press, 2020).
15. Gu, X. *et al.* Mutation screening of the KIF5A gene in Chinese patients with amyotrophic lateral sclerosis. *J. Neurol. Neurosurg. Psychiatry* **90**, 245–246 (2019).
16. Naruse, H. *et al.* Splice-site mutations in KIF5A in the Japanese case series of amyotrophic lateral sclerosis. *Neurogenetics* **22**, 11–17 (2021).
17. van Rheenen, W. *et al.* Common and rare variant association analyses in amyotrophic lateral sclerosis identify 15 risk loci with distinct genetic architectures and neuron-specific biology. *Nat. Genet.* **53**, 1636–1648 (2021).
18. Scaber, J. *et al.* Advantages of routine next-generation sequencing over standard genetic testing in the amyotrophic lateral sclerosis clinic. *Eur. J. Neurol.* **30**, 2240–2249 (2023).
19. Zhang, K. *et al.* Mutation analysis of KIF5A in Chinese amyotrophic lateral sclerosis patients. *Neurobiol. Aging* **73**(229), e1-229. e4 (2019).
20. He, J. *et al.* Whole-exome sequencing identified novel KIF5A mutations in Chinese patients with amyotrophic lateral sclerosis and Charcot-Marie-Tooth type 2. *J. Neurol. Neurosurg. Psychiatry* **91**, 326–328 (2020).
21. Tunca, C. *et al.* Revisiting the complex architecture of ALS in Turkey: Expanding genotypes, shared phenotypes, molecular networks, and a public variant database. *Hum. Mutat.* **41**, e7–e45 (2020).
22. Chen, Y.-P. *et al.* Role of genetics in amyotrophic lateral sclerosis: A large cohort study in Chinese mainland population. *J. Med. Genet.* **59**, 840–849 (2022).
23. Liu, Z. *et al.* Mutation spectrum of amyotrophic lateral sclerosis in Central South China. *Neurobiol. Aging* **107**, 181–188 (2021).
24. Grassano, M. *et al.* Systematic evaluation of genetic mutations in ALS: A population-based study. *J. Neurol. Neurosurg. Psychiatry* **93**, 1190–1193 (2022).
25. Dulski, J., Strongosky, A. J., Al-Shaikh, R. H. & Wszolek, Z. K. Expanding the spectrum of KIF5A mutations-case report of a large kindred with familial ALS and overlapping syndrome. *Amyotroph. Lateral Scler. Frontotemporal Degener.* **24**, 347–350 (2023).
26. Pant, D. C. *et al.* ALS-linked KIF5A ΔExon27 mutant causes neuronal toxicity through gain-of-function. *EMBO Rep.* https://doi.org/10.15252/embr.202154234 (2022).
27. Nakano, J., Chiba, K. & Niwa, S. An ALS-associated KIF5A mutant forms oligomers and aggregates and induces neuronal toxicity. *Genes Cells* **27**, 421–435 (2022).
28. Soustelle, L. *et al.* ALS-associated KIF5A mutation causes locomotor deficits associated with cytoplasmic inclusions, alterations of neuromuscular junctions, and motor neuron loss. *J. Neurosci.* **43**, 8058–8072 (2023).
29. Baron, D. M. *et al.* ALS-associated KIF5A mutations abolish autoinhibition resulting in a toxic gain of function. *Cell Rep.* **39**, 110598 (2022).
30. Carrington, G. *et al.* A multiscale approach reveals the molecular architecture of the autoinhibited kinesin KIF5A. *J. Biol. Chem.* **300**, 105713 (2024).
31. Richards, S. *et al.* Standards and guidelines for the interpretation of sequence variants: A joint consensus recommendation of the American College of Medical Genetics and Genomics and the Association for Molecular Pathology. *Genet. Med.* **17**, 405–424 (2015).
32. Chen, S. *et al.* A genomic mutational constraint map using variation in 76,156 human genomes. *Nature* **625**, 92–100 (2024).
33. Baux, D. *et al.* MobiDetails: Online DNA variants interpretation. *Eur. J. Hum. Genet.* **29**, 356–360 (2021).

34. Kopanos, C. *et al.* VarSome: The human genomic variant search engine. *Bioinformatics* **35**, 1978–1980 (2019).
35. Brand, A. H., Manoukian, A. S. & Perrimon, N. Ectopic expression in Drosophila. *Methods Cell Biol.* **44**, 635–654 (1994).
36. Mahr, A. & Aberle, H. The expression pattern of the Drosophila vesicular glutamate transporter: A marker protein for motoneurons and glutamatergic centers in the brain. *Gene Express. Patterns* **6**, 299–309 (2006).
37. Menon, K. P., Carrillo, R. A. & Zinn, K. Development and plasticity of the Drosophila larval neuromuscular junction. *Wiley Interdiscip. Rev. Dev. Biol.* **2**, 647–670 (2013).
38. Wagh, D. A. *et al.* Bruchpilot, a protein with homology to ELKS/CAST, is required for structural integrity and function of synaptic active zones in Drosophila. *Neuron* **49**, 833–844 (2006).
39. Budnik, V. *et al.* Regulation of synapse structure and function by the Drosophila tumor suppressor gene dlg. *Neuron* **17**, 627–640 (1996).
40. Danella, E. B. & Keller, L. C. A simple neuronal mechanical injury methodology to study Drosophila motor neuron degeneration. *J. Vis. Exp.* https://doi.org/10.3791/56128 (2017).
41. Hurd, D. D. & Saxton, W. M. Kinesin mutations cause motor neuron disease phenotypes by disrupting fast axonal transport in Drosophila. *Genetics* **144**, 1075–1085 (1996).
42. Martin, M. *et al.* Cytoplasmic dynein, the dynactin complex, and kinesin are interdependent and essential for fast axonal transport. *Mol. Biol. Cell* **10**, 3717–3728 (1999).
43. Campbell, P. D. *et al.* Unique Function of Kinesin Kif5A in Localization of Mitochondria in Axons. *Journal of Neuroscience* **34**, 14717–14732 (2014).
44. Pilling, A. D., Horiuchi, D., Lively, C. M. & Saxton, W. M. Kinesin-1 and Dynein are the primary motors for fast transport of mitochondria in Drosophila motor axons. *Mol. Biol. Cell* **17**, 2057–2068 (2006).
45. Chiba, K., Ori-McKenney, K. M., Niwa, S. & McKenney, R. J. Synergistic autoinhibition and activation mechanisms control kinesin-1 motor activity. *Cell Rep* **39**, 110900 (2022).
46. McGuire, S. E., Le, P. T., Osborn, A. J., Matsumoto, K. & Davis, R. L. Spatiotemporal rescue of memory dysfunction in Drosophila. *Science* **302**, 1765–1768 (2003).
47. Neilson, S., Robinson, I., Clifford Rose, F. & Hunter, M. Rising mortality from motor neurone disease: An explanation. *Acta Neurol. Scand.* **87**, 184–191 (1993).
48. Her, Y., Pascual, D. M., Goldstone-Joubert, Z. & Marcogliese, P. C. Variant functional assessment in Drosophila by overexpression: What can we learn?. *Genome* https://doi.org/10.1139/gen-2023-0135 (2024).
49. Guo, X. *et al.* The GTPase dMiro is required for axonal transport of mitochondria to Drosophila synapses. *Neuron* **47**, 379–393 (2005).
50. Verstreken, P. *et al.* Synaptic mitochondria are critical for mobilization of reserve pool vesicles at Drosophila neuromuscular junctions. *Neuron* **47**, 365–378 (2005).
51. Hirokawa, N. & Takemura, R. Molecular motors and mechanisms of directional transport in neurons. *Nat. Rev. Neurosci.* **6**, 201–214 (2005).
52. Guillaud, L., El-Agamy, S. E., Otsuki, M. & Terenzio, M. Anterograde axonal transport in neuronal homeostasis and disease. *Front. Mol. Neurosci.* **13**, 556175 (2020).
53. Karle, K. N., Möckel, D., Reid, E. & Schöls, L. Axonal transport deficit in a KIF5A(-/-) mouse model. *Neurogenetics* **13**, 169–179 (2012).
54. Neisch, A. L., Avery, A. W., Machamer, J. B., Li, M. & Hays, T. S. Methods to identify and analyze gene products involved in neuronal intracellular transport using Drosophila. *Methods Cell Biol.* **131**, 277–309 (2016).
55. Castellanos-Montiel, M. J., Chaineau, M. & Durcan, T. M. The neglected genes of ALS: Cytoskeletal dynamics impact synaptic degeneration in ALS. *Front. Cell Neurosci.* **14**, 594975 (2020).
56. Liu, X. & Henty-Ridilla, J. L. Multiple roles for the cytoskeleton in ALS. *Exp. Neurol.* **355**, 114143 (2022).
57. Yasuda, K., Clatterbuck-Soper, S. F., Jackrel, M. E., Shorter, J. & Mili, S. FUS inclusions disrupt RNA localization by sequestering kinesin-1 and inhibiting microtubule detyrosination. *J. Cell Biol.* **216**, 1015–1034 (2017).
58. Oberstadt, M., Claßen, J., Arendt, T. & Holzer, M. TDP-43 and cytoskeletal proteins in ALS. *Mol. Neurobiol.* **55**, 3143–3151 (2018).
59. Shi, P., Ström, A.-L., Gal, J. & Zhu, H. Effects of ALS-related SOD1 mutants on dynein- and KIF5-mediated retrograde and anterograde axonal transport. *Biochim. Biophys. Acta* **1802**, 707–716 (2010).
60. Williamson, T. L. & Cleveland, D. W. Slowing of axonal transport is a very early event in the toxicity of ALS-linked SOD1 mutants to motor neurons. *Nat. Neurosci.* **2**, 50–56 (1999).
61. Fumagalli, L. *et al.* C9orf72-derived arginine-containing dipeptide repeats associate with axonal transport machinery and impede microtubule-based motility. *Sci. Adv.* **7**, eabg3013 (2021).
62. Goutman, S. A., Chen, K. S., Paez-Colasante, X. & Feldman, E. L. Emerging understanding of the genotype–phenotype relationship in amyotrophic lateral sclerosis. *Handb. Clin. Neurol.* **148**, 603–623 (2018).
63. McCann, E. P. *et al.* Evidence for polygenic and oligogenic basis of Australian sporadic amyotrophic lateral sclerosis. *J. Med. Genet.* https://doi.org/10.1136/jmedgenet-2020-106866 (2020).
64. Van Daele, S. H., Masrori, P., Van Damme, P. & Van Den Bosch, L. The sense of antisense therapies in ALS. *Trends Mol. Med.* **30**, 252–262 (2024).
65. Imlach, W. & McCabe, B. D. Electrophysiological methods for recording synaptic potentials from the NMJ of Drosophila larvae. *J. Vis. Exp.* https://doi.org/10.3791/1109 (2009).
66. Devambez, I. *et al.* Identification of DmTTLL5 as a major tubulin glutamylase in the Drosophila nervous system. *Sci. Rep.* **7**, 16254 (2017).

Acknowledgements

This work was supported by Institut National de la Santé et de la Recherche Médicale and Association pour la Recherche sur la Sclérose Latérale Amyotrophique (Grants R19101FF and R21093FF). We thank the Bloomington Stock Center and the DSHB for providing fly lines and antibodies, respectively. We also thank the Montpellier MRI imaging platform and all members of the laboratory for fruitful discussion and support.

Author contributions

S.L., C.R., and L.S. designed research; S.L., F.A., V.B., C.G. and L.S. performed research; S.L. and L.S. analyzed data; S.L., C.G., C.R., and L.S. wrote the paper.

Competing interests

The authors declare no competing interests.

Additional information

Supplementary Information The online version contains supplementary material available at https://doi.org/10.1038/s41598-024-70543-y.

Correspondence and requests for materials should be addressed to S.L. or L.S.

Reprints and permissions information is available at www.nature.com/reprints.

Publisher's note Springer Nature remains neutral with regard to jurisdictional claims in published maps and institutional affiliations.